



Adsorption of Sodium in an Aqueous Solution in Activated Date Pits

Zakaria Rahal^{1*}, Abderrahmane Khechekhouche², Ayoub Barkat³, Smolyanichenko Alla Sergeevna¹, Chekima Hamza¹.

¹ Department of Water Supply and Sanitation, Don State Technical University, 344000 Rostov-on-Don, Russia.

² Renewable Energy Research Unite in Arid Zones, University of El-Oued, 3900 El Oued, Algeria.

³ Department of Landscape Protection and Environmental Geography, University of Debrecen, 4032 Debrecen, Hungary.

*Correspondence: E-mail: zakariarhl@yahoo.com

ABSTRACT

The use of acid-activated local date pits from Algeria's Oued Souf region for reducing water salinity by removing sodium. The raw and activated date pits were characterized using XRD, FTIR, SEM, and BET. The study used these materials to adsorb sodium from aqueous water, with the effects of activation time, initial sodium concentration, adsorption time, and pH of the solution on sodium removal being investigated. The specific surface area of natural date pits was found to be 645.46 m²/g, while activated date pits had a maximum of 825.03 m²/g. The maximum sodium adsorption capacity was observed at an adsorption time of 90 min, Na⁺ concentration of 600 mg/L, solution pH of 9.0, and adsorbent dosage of 0.1 g. The equilibrium data obtained from the experiment were analyzed using Langmuir and Freundlich isotherm models. The findings revealed that among the isotherm models examined, the Freundlich isotherm model demonstrated the strongest fit, exhibiting a high correlation coefficient of 0.999. Furthermore, the adsorption kinetics were investigated through the analysis of the pseudo-first-order and pseudo-second-order models, and the results indicated that the pseudo-second-order model provided the most suitable fit, with a correlation coefficient of 0.996.

ARTICLE INFO

Article History:

Submitted/Received 12 Jan 2023

First Revised 01 Apr 2023

Accepted 28 Jun 2023

First Available online 03 Jul 2023

Publication Date 01 Dec 2023

Keyword:

Correlation coefficient,

Isotherm,

Kinetics,

Sodium adsorption.

1. INTRODUCTION

Water is an incredibly important natural resource, and it plays a critical role in sustaining life on Earth. Only a small portion of the Earth's water is freshwater, and even less of it is accessible for human use. This has led to concerns about water scarcity in many parts of the world, particularly as the global population continues to grow and demand for freshwater increases. To address these challenges, it is important to take steps to manage our water resources sustainably. This might involve promoting conservation and efficiency, investing in infrastructure to improve access to water, and exploring new technologies for desalination or water reuse (Barkat et al., 2022).

Groundwater is an important source of freshwater for many communities around the world, but in some regions, the quality of groundwater is declining due to increasing salinity levels. Groundwater salinity can be caused by a variety of factors, both natural and human-made.

Some of the natural factors that can contribute to groundwater salinity include rock weathering, which can release minerals into the water and increase its salinity, and evaporation, which can cause water to become more saline if the rate of evaporation exceeds the rate of replenishment.

Over time, high levels of salinity can make groundwater unsuitable for human use and harm ecosystems that depend on freshwater. To address this challenge, it is important to manage groundwater resources sustainably, by monitoring water quality, promoting conservation and efficiency, and implementing practices that minimize salt and mineral leaching into the groundwater (Barkat et al., 2022; Barkat et al., 2021; Sadasivuni et al., 2019).

Solar-powered groundwater treatment is a promising technology that can provide clean and safe water to communities in

remote and underserved areas. However, it should be carefully evaluated and designed to ensure its effectiveness and sustainability. Groundwater treatment using solar energy is a sustainable and cost-effective method of purifying contaminated water.

Solar-powered water treatment systems can be used to remove a variety of contaminants such as bacteria, viruses, heavy metals, and chemicals from groundwater sources. There are different types of solar-powered water treatment systems, but the most common ones are solar stills and solar photovoltaic (PV) systems.

Solar stills use solar energy to evaporate water and collect the condensed vapor, which is free of contaminants. On the other hand, solar PV systems use solar panels to generate electricity, which can power pumps, filters, and other water treatment equipment (Khelassi-Sefaoui et al., 2021; Miloudi et al., 2022; Khechekhouche et al., 2020; Khechekhouche et al., 2019; Wakeel et al., 2011; Jennings, 1976).

Water salinity is a major global issue caused by the presence of dissolved salts in water, affecting millions of people worldwide. High levels of salt can make water unsuitable for human consumption, irrigation, and industrial use, and can also lead to negative impacts on soil fertility and reduced crop yields.

Water salinity can be caused by natural processes or human activities such as agriculture, industrial activities, and urbanization. To address water salinity issues, various strategies such as desalination, water management practices, and soil and water conservation practices can be employed.

Overall, addressing water salinity requires a collaborative effort from stakeholders to ensure access to safe and sustainable water sources (Remoundaki et al., 2016; Munns et al. 2002).

The accumulation of salt in the water can alter soil structure, reducing its ability to hold water and increasing the risk of erosion. This can further exacerbate the negative impacts of high sodium levels on soil health and fertility. To mitigate the effects of high sodium levels in water on soil health, several strategies can be employed, such as soil amendments, crop rotation, and irrigation management.

Soil amendments, such as gypsum, can help to displace excess sodium in the soil, while crop rotation can help to restore soil health by reducing salt buildup and promoting nutrient cycling.

Irrigation management practices, such as the use of drip irrigation or the recycling of drainage water, can also help to reduce the amount of salt entering the soil. Overall, managing the impacts of high sodium levels in water on soil health is crucial for ensuring sustainable agriculture and protecting ecosystem health (Zamanzadeh-Nasrabadi *et al.*, 2023; Mohanavelu *et al.*, 2021; Agudelo *et al.*, 2016; Musie *et al.*, 2022).

As an economical method, adsorption is a widely used technique for both alkalinity and salt removal. The process involves the attachment of ions or molecules to the surface of a solid material known as an adsorbent. Local and affordable adsorbents such as rice husk, sugarcane bagasse, coconut coir, and zeolites have been investigated for the removal of calcium, magnesium, and sodium ions from water.

Additionally, activated carbon and ion exchange resins can be used as adsorbents, although they are more expensive than natural adsorbents. However, they can be regenerated and reused, making them a more sustainable option in the long run. The choice of an adsorbent depends on factors such as cost, availability, and the desired degree of reduction in alkalinity (Musie *et al.*, 2023; Kermerchou *et al.*, 2022; Brihmat *et al.*, 2022; Bumajdad *et al.*, 2023).

Plants or plant parts have been studied as a natural and sustainable solution for water

treatment, with the ability to absorb and accumulate pollutants from water. Water hyacinth, duckweed, reed, and cattail are some of the most commonly studied plants for water treatment, with effectiveness depending on factors such as the type of pollutants present and environmental conditions.

Plant-based water treatment can be used in a variety of settings, from small-scale household systems to large-scale wastewater treatment plants, and can be combined with other treatment methods to improve overall efficiency. Overall, the use of plants for water treatment is a promising approach to sustainable and cost-effective water treatment (Azam *et al.*, 2022; Azmi *et al.*, 2020; Kollannur *et al.*, 2019; Toor *et al.*, 2012; Theydan *et al.*, 2012).

Date pits have been investigated as a low-cost adsorbent for the removal of metal ions and other impurities from water. Date pits are an agricultural waste product and are abundant in regions where dates are grown. The use of date pits as an adsorbent is a sustainable approach to water treatment that can reduce waste and provide an affordable solution for communities with limited resources.

Studies have shown that date pits can effectively remove metal ions such as lead, copper, and zinc from water. Factors such as pH, contact time, and the concentration of metal ions in the water exert an influence on the adsorption process. Overall, the use of date pits as an adsorbent is a promising approach to low-cost and sustainable water treatment (Mari *et al.*, 2018; Rahal *et al.*, 2022a; Rahal *et al.*, 2022b, Rahal *et al.*, 2022c; Rahal *et al.*, 2021).

This work aimed to explore the potential of locally available date pits as an affordable and sustainable solution for reducing water salinity. The study focused on date pits from the Oued Souf region in Algeria, which were chemically and thermally activated for better performance. The modified date pits were then tested for their ability to remove

sodium from water, and several parameters were studied to optimize the process, including activation time, initial introduced sodium concentration, time of the adsorption, solution's pH, and the dosage of the adsorbent.

2. METHODS

In scientific experiments as shown in **Figure 1**, it is important to use high-quality chemicals to ensure accurate and reproducible results. Therefore, the chemicals used were of research-grade quality, including sodium hydroxide (NaOH), sodium chloride (NaCl), sulfuric acid (H₂SO₄), and hydrochloric acid (HCl).

These chemicals are commonly used in research studies and have known properties and characteristics that make them suitable for a variety of applications.

Ion exchange is the process through which deionized water, also known as purified water, is produced by effectively removing all mineral ions from it. This type of water is preferred in scientific experiments because it is free from impurities and contaminants that could potentially affect the results.

The date pits used in the study were collected from the Oued Souf region in Algeria. This region is known for its

production of high-quality dates. By utilizing this agricultural waste product, we were able to explore a potentially low-cost and sustainable solution for reducing water salinity. The sample was then analyzed, and the adsorption process was measured using equations under some parameters. The parameters are presented in **Table 1**.

2.1. Adsorbent Preparation

The date pits were processed without activation by stirring them in a cylindrical container with running tap water for 15-20 min at a temperature of 16-18°C. The date pits were then placed on an inclined moisture-resistant surface to remove dripping liquids for 20-30 min before being laid out on a flat absorbent surface to dry at room temperature of 30-36°C for 24 hours. Once the date pits were completely dry, they were crushed, and the crushed mixture was divided into fractions of size \emptyset (0.45/0.63 mm).

To activate the date pits, they were pretreated and then added to an Erlenmeyer flask containing 250 mL of H₂SO₄ solution with a concentration of 1 M. The mixture was agitated continuously at 250 rpm using a magnetic stirrer, and the activation time was varied from 5 to 20 min.

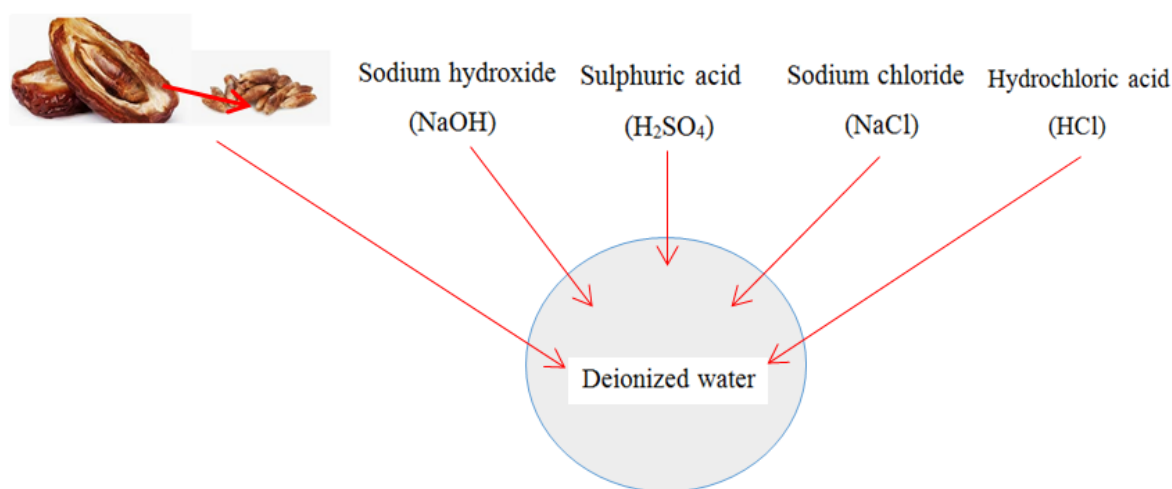


Figure 1. Experiment components.

Table 1. Nomenclature.

Symbol	Note
X	Mass fraction of moisture
m_1	Mass of the initial adsorbent with a glass (g)
m	Mass of the glass (g)
m_0	Mass of the dried adsorbent with a glass (g)
q_t	Amount of sodium per unit mass of date pits (mg/g)
C_0	Initial sodium concentration (mg/L) initial sodium concentration (mg/L)
C_e	Equilibrium dye concentration (mg/L)
V	Volume of salt solution
m_d	Date pits mass (g)
q_e	Amount of adsorbate adsorbed per unit mass of adsorbent used (mg/g)
K_l	Langmuir constant related to the energy of adsorption (L/mg)
q_m	Maximum amount of adsorbate adsorbed per unit mass of adsorbent to form a complete monolayer on the surface of adsorbent (mg/g)
C_e	Equilibrium liquid phase concentration and adsorbate at different periods
K_f	Adsorption capacity of the sorbent
n	Freundlich constant
q_e	Amount of adsorbate adsorbed at equilibrium (mg/g)
q_t	Amount of adsorbate adsorbed at the time (mg/g)
k	Rate constant of the adsorption process
k_1	Pseudo-first-order rate constant
t	Time (min)
bt	Constant related to the heat of sorption [J/mol]
At	Temkin equilibrium binding constant [L/mg]
K_j	Jovanovich constant [L/mg]
Kad	Dubinin-Radushkevich isotherm constant related to adsorption energy [mol ² /J ²]
ε	Polanyi potential constant related to the Dubinin-Radushkevich model
qSd	Dubinin-Radushkevich theoretical isotherm saturation capacity [mg/g]
E	Adsorbate energy per molecule is the energy needed to remove the molecule from the surface
KH	Halsey constant
nH	Hill cooperativity coefficient of the binding interaction
Kr	Redlich-Peterson isotherm constant [L/g]
ar	Redlich-Peterson isotherm constant [L/mg]
g	Redlich-Peterson isotherm exponent
α	Initial adsorption rate [mg/ min]
β	Desorption constant [g/mg]

The clear solution at the top of the mixture was decanted once it had settled, and the remaining particles were repeatedly rinsed with distilled water until the pH of the top solution reached 4.5 to 5.0.

The activated date pits were then placed in a freezer at -10°C for 9 hours before being dried in an oven at 105°C for 12 hours to obtain the final samples.

It is worth noting that the washing steps were important to remove any dissolvable

impurities from the date pits, ensuring that the activated samples were as pure as possible. Furthermore, the use of acid activation with H₂SO₄ was likely intended to increase the surface area and porosity of the date pits, making them more effective at adsorbing sodium from the water. Overall, the process of preparing the date pits sample involved several carefully controlled steps to obtain a pure and well-activated sample for subsequent testing.

2.2. Characterization of Date Pits

The ash content of the adsorbent was determined by weighing 2 g of the dry matter, placing it in ceramic evaporation dishes, and burning it at 600°C within 2 hours. The ash weight was subtracted from the dry weight to calculate the ash content. To determine the moisture content of the adsorption material, a 2 g sample was weighed and poured into a cup (which was previously weighed). The sorbent was dried in an oven at 105°C for 1 hour, and the cup with the sorbent was reweighed after cooling to determine the moisture content. These methods were used to ensure accurate and reliable measurements of the physical properties of the adsorbent material.

The mass fraction of moisture was calculated by the Equation (1):

$$X = \frac{(m_1 - m_0)}{m_0 - m} 100 \quad (1)$$

The determination of the bulk density of the adsorbent involved pouring it in 20 mL increments into a 100-mL cylinder and tapping it against a wooden disk. According to GOST 17219-71, the total pore volume was determined, and Brunauer-Emmett-Teller was used to calculate the specific surface areas of the raw and activated date pits. FTIR was used to study the functional group of the adsorbents, and field emission scanning electron microscopy (SEM) was used to look at the morphological properties. Utilizing an X-ray diffractometer (XRD), the crystallinities of the adsorbents were investigated, and the compositions were identified by chemical analysis.

Overall, various techniques were used to characterize the properties of the adsorbent, including its bulk density, pore volume, surface area, functional group, morphology, crystallinity, and composition.

2.3. Adsorption Performance

The point of zero charges for the date pits was achieved first, and then batch

adsorption tests were conducted to evaluate the activated date pits' adsorption efficiency. In 250-mL Erlenmeyer flasks with a 50-mL working volume and starting sodium concentrations of 100, 300, and 600 mg/L (as Na⁺), adsorption tests were carried out. Based on the point of zero charge analysis, the pH of the solutions was changed to 8 using NaOH and H₂SO₄. Then, activated date pits weighing 0.2, 0.1, and 0.05 g were added to each salt solution, and the mixture was mixed for 180 min at room temperature in an isothermal water bath shaker. After filtering, the solutions' salt content was tested with a flame photometer. The amount of sodium adsorbed on the date pits was calculated using Equation (2).

$$q_t = \frac{(c_0 - c_e)v}{m} \quad (2)$$

2.4. Data of Adsorption Equilibrium

The study investigated the effectiveness of several isotherms, in describing the adsorption of sodium on date pits. Adsorption isotherms depict the relationship between the concentration of a solute in the liquid phase and its corresponding concentration within the adsorbent material, specifically at a given temperature.

As per the Langmuir adsorption model, the maximum adsorption occurs when a saturated monolayer of solute molecules is established on the surface of the adsorbent. To establish the equilibrium relationship between sodium concentration and its adsorption on date pits, the experimental data were analyzed using two models. The Langmuir model, represented by Equation (3), was employed for this purpose.

$$\frac{c_e}{q_e} = \frac{1}{q_m k_l} + \frac{1}{q_m c_e} \quad (3)$$

Freundlich isotherm model is given by Equation (4):

$$\ln q_e = \ln k_f + \frac{1}{n} \ln c_e \quad (4)$$

The Temkin isotherm equation assumes that the heat of adsorption of all the

molecules in the layer decreases linearly rather than logarithmically as equilibrium adsorption capacity increases because the bt factor is related to adsorbent-adsorbate interactions (Reyhaneh *et al.*, 2015).

The adsorption is characterized by a uniform distribution of the binding energies, up to some maximum binding energy.

The model is given by Equation (5)

$$qe = bt \ln AtCe \quad (5)$$

The model of an adsorption surface considered by Jovanovich is essentially the same as that considered by Langmuir. But the Jovanovich equation has a slower approach toward saturation than the Langmuir equation. The Jovanovich model is shown as Equation (6) (Nandiyanto *et al.*, 2020a).

$$qe = qmax(1 - e^{-KjCe}) \quad (6)$$

Dubinin Radushkevich's model is a semiempirical equation in which the adsorption of this model follows the mechanism of pore filling. This model assumes that a multilayer character, which involves Van der Waal's forces, can be applied to the physical adsorption processes. This isotherm model is usually applied to distinguish the physical and chemical adsorption of adsorbate ions.

The Dubinin-Radushkevich isotherm model can be computed by Equations (7) and (8)

$$qe = qsd e^{(-Kad\varepsilon^2)} \quad (7)$$

$$E = 1/(2\sqrt{\beta}) \quad (8)$$

where E is the adsorbate energy per molecule as the energy needed to remove molecules from the surface.

- If $E < 8$ kJ/mol, physical adsorption;
- If $8 < E < 168$ kJ/mol, chemical adsorption.

Halsey model is suitable for multilayer adsorption as well as heterogeneous surfaces in which the adsorption heat is non-uniformly distributed. The Halsey

model can be shown as Equation (9) (Nandiyanto *et al.*, 2020b).

$$qe = e^{((\ln KH - \ln ce)/nH)} \quad (9)$$

The Redlich-Peterson isotherm model features Freundlich and Langmuir isotherm models with three parameters, and the mechanism of adsorption is a hybrid and does not follow ideal monolayer adsorption. This model can be applied either in homogeneous or heterogeneous systems.

The Redlich-Peterson isotherm model can be computed by Equation (10).

$$qe = Krce/(1 + Ar [ce]^g) \quad (10)$$

2.5. Adsorption Kinetics

The pseudo-second-order kinetic model assumes that the rate of adsorption is proportional to the square of the number of unoccupied sites on the adsorbent surface. By fitting the experimental data to these models, the rate constants and equilibrium adsorption capacities were determined, providing insights into the kinetics and mechanisms of sodium adsorption onto activated date pits (Azmi *et al.*, 2020a).

Equation (11) illustrates the pseudo-first-order kinetic model.

$$\ln(q_e - q_t) = \ln q_e - k_1 t \quad (11)$$

The pseudo-second-order model expresses that the rate of adsorption, or the amount of adsorbate adsorbed per unit of time, is directly proportional to the square of the number of unoccupied sites on the surface of the adsorbent and the concentration of the adsorbate remaining in the solution. Mathematically, the model can be represented in Equation (12):

$$\frac{t}{q_t} = \frac{1}{k_2 q_e^2} + \frac{1}{q_e} \quad (12)$$

Elovich kinetic model is used to evaluate the mechanisms and dynamics of the adsorption process. The Elovich kinetic model can be computed by Equation (13).

$$q_t = \frac{1}{\beta} \ln(\alpha \beta t + 1) \quad (13)$$

3. RESULTS AND DISCUSSION

3.1. Characteristics of the Raw and Activated Date Pits

Table 2 summarizes the characteristics of date stones. The most important properties are the surface area and total pore volume, ΣV . The surface area of date pits is 675.46 m^2/g , and that of activated date pits is 825.08 m^2/g . The total pore volume, ΣV , of the date pits, is 0.962 cm^3/g , whereas that of the activated date pits is 1.468 cm^3/g . The bulk density of the raw and activated date pits is 0.321 g/cm^3 and 0.324 g/cm^3 , respectively. The ash content of the date pits is 11.25%, and that of activated date pits is 11.12%. The moisture content of the raw and activated date pits is 18.54% and

10.08%, respectively, which is lower than what was reported by the author [32, 33].

Figures 2 and **3** illustrate the *SEM* images of the date pits before and after activation, respectively. The surface of the date pits appears relatively rough, with small pores. After chemical activation, the number of pores increases, while the size of the pores remains relatively unchanged. The exchangeable cations, such as (K^+ , Na^+ , and Ca^{2+}) between the layers are substituted with hydrogen ions during activation, leading to more pores and, thus, a larger surface area. Previous research has reported that impregnation with H_2SO_4 has a significant impact on increasing specific surface area and the development of micropores.

Table 2. Characteristics of the raw and activated date pits.

Characteristic	Raw Date Pits	Activated Date Pits
Bulk density (g/cm^3)	0.321	0.324
Ash content (%)	11.25	11.12
Moisture content (%)	18.54	10.08
Surface area (m^2/g)	645.46	825.03
Total pore volume, ΣV (cm^3/g)	0.962	1.468

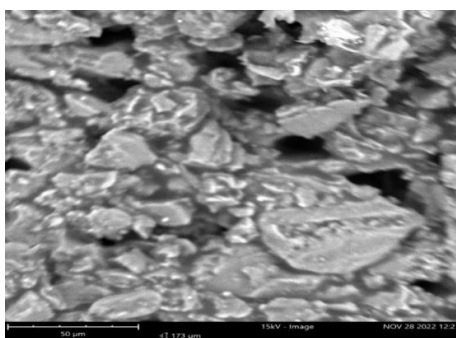


Figure 2. SEM images of raw date pits.

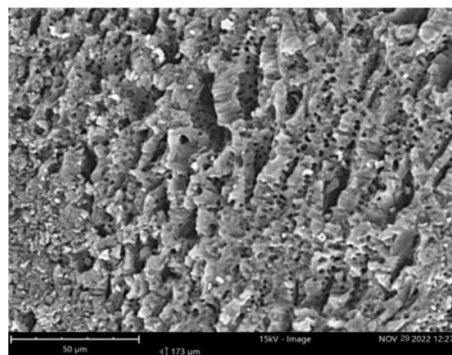


Figure 3. SEM images of activated date pits.

3.2. The Date Pits Chemical Composition, Both Raw and Activated

Table 3 lists the chemical element of date pits, both raw and H₂SO₄-activated. The chemical analysis of the date pits was conducted using standard chemical methods, with the moisture content of the date stones being excluded from the analysis. The results show that the silica content slightly increased after acid treatment, while the percentage of calcium also increased. On the other hand, the other oxides composition tended to decrease after activation.

3.3. Analysis of FTIR

The FTIR spectra of the raw date pits, H₂SO₄-activated date pits, and after sodium adsorption are presented in **Figure 4**. The spectra show that the date pits are dominated by the montmorillonite group, as indicated by the peaks in the lower wavenumber regions (1700-800 cm⁻¹).

The adsorbent exhibits a wide-ranging peak ranging from 3518-3630 cm⁻¹, which is attributed to the lignocellulose peaks of -NH, -OH, or both -NH₂ and OH. The peak at 1675 cm⁻¹ corresponds to the OH deformation mode of water, while the peak at around 1133 cm⁻¹ corresponds to Si-O stretching, indicating the presence of quartz. The FTIR results reveal no significant difference in the surface functional groups between the raw and H₂SO₄-activated date pits. However, after sodium adsorption, a shift in the Si-O stretching peak from 1133 to 1110 cm⁻¹ was observed, indicating ion exchange with Na⁺. The intensities of peaks at 3660 cm⁻¹, 1739 cm⁻¹, and 800 cm⁻¹ increased, indicating interaction with Na⁺ in these regions. The negative surface charge of the adsorbent can facilitate physical attachment and substitution of the displaced ions from the intermediate structure, providing other sites for sodium ion adsorption.

Table 3. Chemical elements of pits at the dry base level.

Element	Raw date pits (wt.%)	Activated date pits (wt.%)
C	60.66	62.41
O	29.87	27.63
K	4.61	3.42
Si	1.37	2.65
Ca	2.54	3.67
P	0.95	0.22

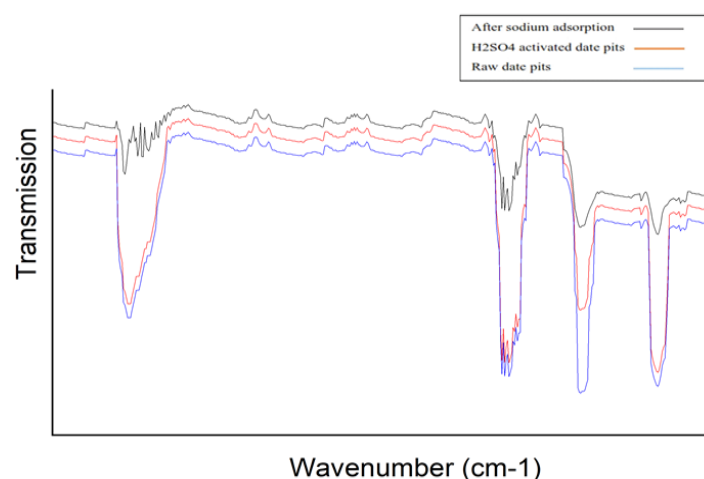


Figure 4. FTIR spectrums of raw, H₂SO₄ activated date pits and after sodium ion adsorptions.

3.4. Point of Zero Charge

The point of zero charges (PZC) of the adsorbents is the pH at which the surface charge of the adsorbent is zero. To determine the PZC, 0.2 g of raw and activated date pits were added to 100 mL solutions with initial pH values ranging from 3.0 to 7.0, and the suspensions were agitated for 24 hours at room temperature with a shaking speed of 120 rpm. The pH was adjusted using 0.1 M NaOH and 0.1 M HCl. After 24 hours, the equilibrium pH was measured, and the pH difference (ΔpH) was calculated using the equation: $\Delta\text{pH} = \text{pH} (1) - \text{pH} (2)$, where pH (1) is the initial pH and pH (2) is the final pH. The intersection of the curve with the horizontal axis at $\Delta\text{pH} = 0$ indicates the PZC. The PZC for raw date pits was found to be 8.0, as shown in **Figure 5**. However, the PZC for activated date pits was found to be 4.0, making it suitable for use as an adsorbent in a varied range of pH operations.

3.5. Adsorption Kinetics

To investigate the sodium adsorption process on the activated date pits, experiments were carried out using different amounts of sorbent samples (0.05, 0.1, and 0.15 g) and different concentrations of Na^+ solution (100, 300, and 600 mg/L) as shown in **Figure 6**. The flasks containing the samples and solutions were stirred with a

magnetic stirrer at 120 rpm at room temperature ($29 \pm 0.5^\circ\text{C}$) for different contact times ranging from 5 to 180 min. After the desired contact time, the solutions were filtered through a blue band filter, and the residual concentrations of sodium ions in the filtrate were measured using a flame photometer. Each experiment was repeated three times to obtain the average value. The adsorption kinetics was determined by analyzing the relationship between the adsorption rate and contact time.

Figure 6 shows the Na^+ adsorption efficiency plotted against contact time and initial concentrations of sodium ions. The results demonstrate that the adsorption process of sodium on activated date pits can be divided into three stages: fast, slow, and equilibrium. During the last stage, which lasts for the first 20 min, the adsorption rate increases rapidly until more than half of the adsorption capacity is reached.

During the Na^+ adsorption process on activated date pits, the adsorption rate decreases in the second (slow) phase, which occurs after 20 min and reaches equilibrium after 90 min. Additionally, it was observed that the adsorption rate increases with increasing initial concentration of Na^+ throughout the study. **Table 4** provides a list of the outcomes and **Figure 7** was generated by utilizing the given values in the nonlinear equations.

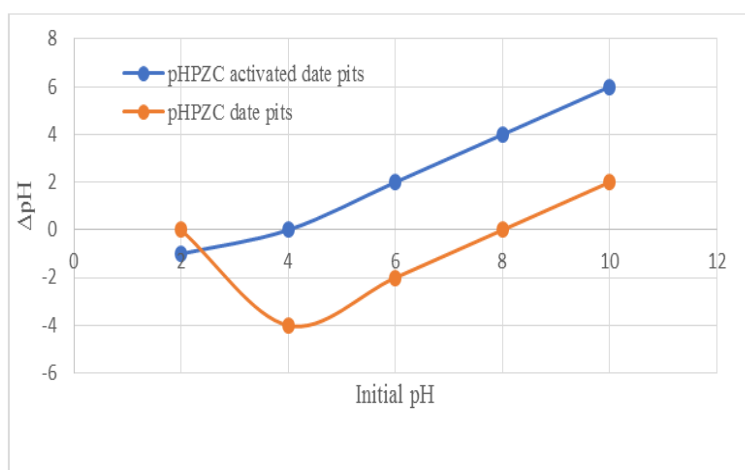


Figure 5. Zero point charges of raw and activated date pits.

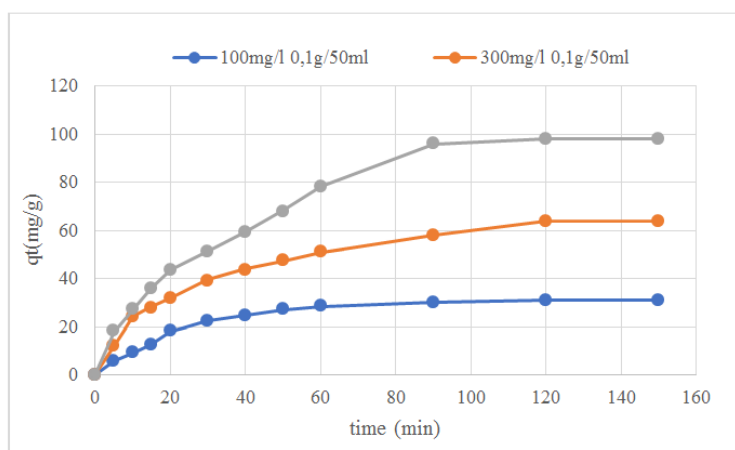


Figure 6. Kinetics of Na⁺ adsorption on date pits.

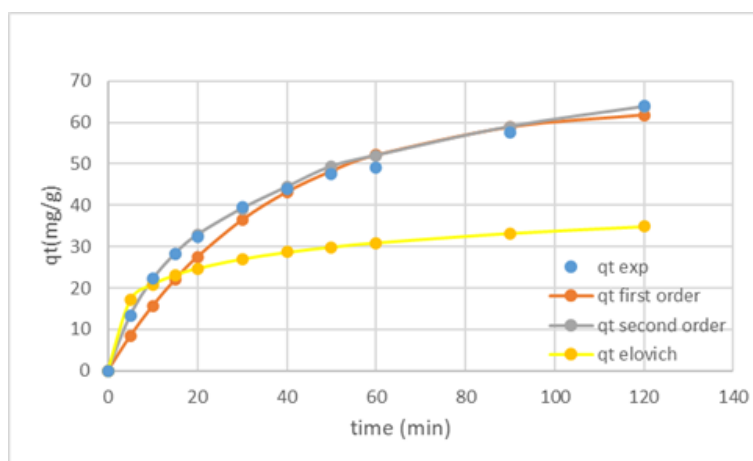


Figure 7. Comparison of Na⁺ adsorption in various kinetic models.

The q_e -equilibrium adsorption capacity (q_e) was estimated using the pseudo-second-order model, and it was discovered that the result was extremely similar to the value determined from the experimental data, as shown in **Table 4**. The experimental kinetic data and the pseudo-second-order model suit each other well, as seen by the

high correlation coefficient value (R^2), which points to surface chemical adsorption as the potential rate-limiting phase. The second-order kinetic model has also been shown to be effective in characterizing the adsorption kinetics of date pit-based adsorbents in earlier investigations.

Table 4. Kinetic model constants.

Kinetic Model	Parameters	Value of Kinetic parameters on a linear fit
Pseudo-first order	Removal potential (q_e)	Exp ^{tal} model 64
	Constant	61.77
	R^2	$k_1 = 0.0287$ 0.967
Pseudo-second order	Removal potential (q_e)	Exp ^{tal} model 64
	Constant	63.74
	R^2	$k_2 = 0.0007$ 0.996
Elovich	Constant	$\alpha = 21.85$
	R^2	0.9802

3.6. Adsorption Isotherms

The dependence of the sodium ion adsorption process on temperature was investigated in this research. Temperature is a crucial factor in the absorption process and plays a significant role in determining the hardware design of the water filtration technology. Langmuir and Freundlich's models were used to analyzing the experimental data, taking into account the fact that the Langmuir isotherms describe the adsorption process in homogeneous regions of the adsorbent body, while the Freundlich isotherms imply adsorption on heterogeneous surfaces with uneven distribution of adsorption centers. To ensure optimal conditions for sodium uptake during the purification stages, the temperature and pH were controlled at $28 \pm 2^\circ\text{C}$ and 8 ± 0.5 , respectively. The correlation coefficients R^2 showed that both the Freundlich and Langmuir models accurately describe the Na^+ adsorption process on activated date pits, with R^2 values greater than 0.98 for all models. **Table 5** and **Figure 8** demonstrate that the Freundlich model exhibited a superior fit to the experimental data

compared to the Langmuir model, as evidenced by a high correlation coefficient (R^2) of 0.99.

The comparison of the Langmuir and Freundlich isotherms suggests that the Na^+ adsorption mechanism consists of two reaction processes occurring predominantly on the surface of the activated date pits, which is consistent with the previously proposed hypothesis. The experimental data show that the Freundlich isotherm more accurately describes the adsorption process than the Langmuir isotherm, indicating a heterogeneous adsorption process.

Several models have been used to analyze the experimental data and conduct a comparison between them, which point to surface chemical adsorption as the potential rate-limiting Phase. The models that were used are Temkin, Dubinin-Radushkevich, Halsey, Redlich-Peterson, and Jovanovich models. **Table 5** and **Figure 8** demonstrate that the Halsey model exhibited a superior fit to the experimental data compared to other models, as evidenced by a high correlation coefficient (R^2) of 0.99.

Table 5. Adsorption isotherm model constants.

Isotherm model		Value of parameters on linear fit to different models	
Type	Value	Note	
Freundlich	KF (mg/g) = 1.562	-	
	$1/n = 0.6509$; $n > 1$	favorability of adsorption process(adsorption occurs normally and is controllable under specific condition)	
	$R^2 = 0.999$	-	
Langmuir	KL (L/mg) = 0.004	Relatively small KL values, indicating that there is a weak interaction between adsorbate and adsorbent.	
	qm (mg/g) = 69.676	-	
	$R^2 = 0.985$	-	
Temkin	$\beta T = 37,128$	$\beta T > 8$ kJ/mol, Chemical Adsorption	
	$R^2 = 0.878$	-	
Dubinin-Radushkevich	qm (mg/g) = 94.886	-	
	E (kJ mol ⁻¹) =11.78	$E > 8$ kJ/mol, Chemical Adsorption	
	$R^2 = 0.839$	-	
Halsey	$KH = 2.003$	-	
	$R^2 = 0.999$	-	
Redlich-Peterson	Kr [L/g] =5,523435	-	
	$g = 1.5573$	-	
	$R^2 = 0.937$	-	
Jovanovich	$Kj = 0.0018$	-	
	$R^2 = 0.878$	-	

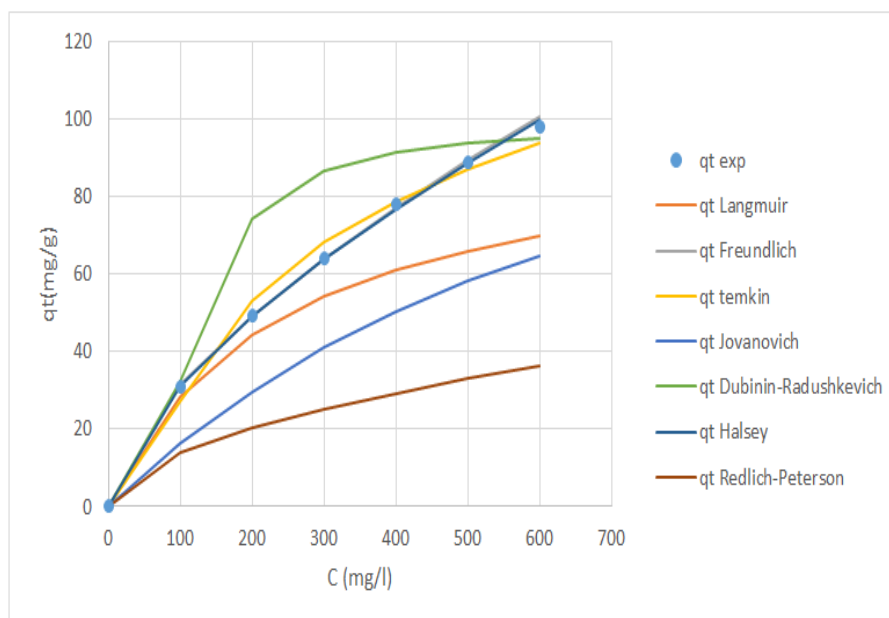


Figure 8. Compares the experimental data for the sorption of Na^+ on the activated date pits with the isotherms models.

3.7. pH Effect of the Solution

50 mL of salt solutions with pH values ranging from 2 to 10 were combined with 0.1 g of date pits for 120 min to investigate the influence of pH on the adsorption of Na^+ . The surface charge of the adsorbent and the ionic forms of metals are both greatly influenced by the pH of the solution. **Figure 9** illustrates how the ability of Na^+ to bind to surfaces rises with pH up to pH 9. At higher pH values, the change in Na^+ adsorption capacity was not significant. The

surface charge of the adsorbent is influenced by the presence of H^+ or OH^- ions in the solution. The surface functional groups on the adsorbent are negatively charged if the pH of the salt solution is above the point of zero charges ($\text{pH}=7$). This causes electrostatic interaction between the positively charged ions, resulting in greater sodium removal. Overall, based on the obtained results, it is suggested that pH plays a crucial role in the adsorption of Na^+ on activated date pits.

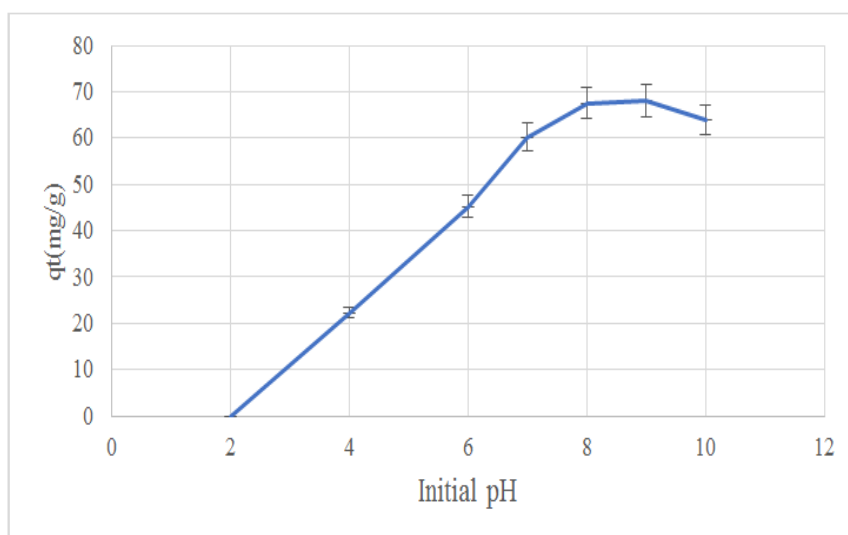


Figure 9. Effect of pH of a solution of Na^+ adsorption on date pits.

4. CONCLUSION

The study explored the potential of activated date pits from Algeria to reduce salinity in water by removing sodium ions. The date pits' surface area was observed to increase during the H₂SO₄ activation process, giving them a maximum sodium adsorption capacity of 98 mg/g. The Freundlich isotherm is best suited to the adsorption equilibrium data, while the pseudo-second-order model best fits the kinetic model. The study also found that pH

and temperature significantly affected the adsorption process, with higher pH values resulting in more effective sodium removal. Overall, the study suggests that activated date pits could be a promising and cost-effective adsorbent for sodium removal in water treatment applications.

5. AUTHORS' NOTE

The authors declare that there is no conflict of interest regarding the publication of this article. The authors confirmed that the paper was free of plagiarism.

6. REFERENCES

- Agudelo, J. A., Cardona, L. C., and Lopez, L. A. (2016). Removal of sodium and chloride ions from aqueous solutions using fique fibers (*Furcraea* spp.). *Water Science and Technology*, 73(5), 1197-1201.
- Azam, M., Hussain, M. A., Iqbal, M., and Khan, A. (2022). Date pits waste as a solid phase extraction sorbent for the analysis of lead in wastewater and for use in manufacturing brick: An eco-friendly waste management approach. *Journal of Saudi Chemical Society*, 26(5), 101519.
- Azmi, S. N. H., Al-Busafi, S. N., and Al-Abri, M. (2020). Adsorptive removal of Pb(II) ions from groundwater samples in Oman using carbonized Phoenix dactylifera seed (Date stone). *Journal of King Saud University-Science*, 32(7), 2931-2938.
- Barkat, A., Bouaicha, F., Bouteraa, O., Mester, T., Ata, B., Balla, D., Rahal, Z., and Szabó, G. (2021). Assessment of complex terminal groundwater aquifer for different use of Oued Souf Valley (Algeria) using multivariate statistical methods, geostatistical modeling, and water quality index. *Water*, 13(11), 1609.
- Barkat, A., Bouaicha, F., Mester, T., Debabeche, M., and Szabó, G. (2022). Assessment of spatial distribution and temporal variations of the phreatic groundwater level using geostatistical modelling: The case of Oued Souf Valley—Southern East of Algeria. *Water*, 14(9), 1415.
- Brihmat, A., Mahcene, H., Bechki, D., Bouguettaia, H., Khechekhouche, A., and Boughali, S. (2022). Energy performance improvement of a solar still system using date and olive kernels: experimental study. *CLEAN - Soil, Air, Water*, 50(12), 2100497.
- Bumajdad, A., Al-Khalidi, M., Jbara, O. A., Khalaf, M., Asghar, H., and Jibril, B. Y. (2023). Surface modification of date palm activated carbonaceous materials for heavy metal removal and CO₂ adsorption. *Arabian Journal of Chemistry*, 16(1), 104403.
- Jennings, D. H. (1976). The effects of sodium chloride on higher plants. *Biological Reviews*, 51(4), 453-486.

- Kermerchou, I., Mahdjoubi, I., Kined, C., Khechekhouche, A., Bellila, A., and Isiordia, G. E. D. (2022). Palm fibers effect on the performance of a conventional solar still. *ASEAN Journal for Science and Engineering in Materials*, 1(1), 29-36.
- Khechekhouche, A., Bouchemal, F., Kaddour, Z., Salim, K., and Miloudi, A. (2020). Performance of a wastewater treatment plant in south-eastern Algeria. *International Journal of Energetica*, 5, 47-51.
- Khechekhouche, A., Driss, Z., and Durakovic, B. (2019). Effect of heat flow via glazing on the productivity of a solar still. *International journal of Energetica*, 4(2), 54-57.
- Khelassi-Sefaoui, A., Zaoui-Djelloul-Daouadji, M., Naili, I., Zaiter, L., Benarima, H., and Khechekhouche, A. (2021). Phytochemical investigation, antibacterial and antioxidant activities of *Sideritis incana* L extracts. *Algerian Journal of Engineering and Technology*, 5, 49-54.
- Kollannur, D., Sridharan, A., and Mariappan, M. (2019). Methodology for determining point of zero salt effect of clays in terms of surface charge properties. *Journal of Materials in Civil Engineering*, 31(12), 04019286.
- Mari, A., Halouane, F., Sehili, T., Chiban, M., and Bensmaili, A. (2018). Effect of structure and chemical activation on the adsorption properties of green clay minerals for the removal of cationic dye. *Applied Sciences*, 8(11), 2302.
- Miloudi, A., Khechekhouche, A., and Kermerchou, I. (2022). Pollution groundwater treatment by solar stills with palm fibers. *JP Journal of Heat and Mass Transfer*, 27, 1-12.
- Mohanavelu, A., Naganna, S. R., and Al-Ansari, N. (2021). Irrigation induced salinity and sodicity hazards on soil and groundwater: An overview of its causes, *Impacts and Mitigation Strategies. Agriculture*, 11(10), 983.
- Munns, R. (2002). Comparative physiology of salt and water stress. *Plant, Cell and Environment*, 25(2), 239-250.
- Musie, G., Abebe, T., and Tekleab, T. (2022). Adsorption of sodium from saline water with natural and acid activated Ethiopian bentonite. *Results in Engineering*, 14, 100440.
- Musie, G., Tekleab, T., and Abebe, T. (2023). Adsorption Studies of Sodium Ions from Aqueous Solution with Natural and Sulfuric Acid-Treated Bean Seed Husk. *Water, Air, and Soil Pollution*, 234(3), 170.
- Nandiyanto, A. B. D., Maryanti, R., Fiandini, M., Ragadhita, R., Usdiyana, D., Anggraeni, S., Wafa, R. A., Abdulkareem. Sh., and Al-Obaidi, A. S. M. (2020). Synthesis of carbon microparticles from red dragon fruit (*Hylocereus undatus*) peel waste and their adsorption isotherm characteristics. *Molekul*, 15(3), 199-209.
- Nandiyanto, A. B. D., Ragadhita, R., and Yunas, J. (2020). Adsorption isotherm of densed monoclinic tungsten trioxide nanoparticles. *Sains Malaysiana*, 49(12), 2881-2890.
- Rahal, Z., and Chekima, H. (2021). Regulation of water quality in urban aquifers in southeastern Algeria in traditions and innovations in construction and architecture. *Construction and Building Technologies*, 5, 626-630.

- Rahal, Z., and Chekima, H. (2022). On the question of heavy metals biosorption on plant sorbents. In Traditions and innovations in construction and architecture. *Construction and Building Technologies*, 6, 654-661.
- Rahal, Z., Chekima, H., and Serpokrylov, N. S. (2022a). The use of palm leaves as a potential adsorbent for wastewater treatment. *Engineering and Construction Bulletin of the Caspian Sea*, 3(41), 37-43.
- Rahal, Z., Chekima, H., Smolyanichenko, A. S., and Serpokrylov, N. S. (2022b). The use of date pits as a potential adsorbent for groundwater treatment. *Engineering and Construction Bulletin of the Caspian Sea*, 4(42), 26-29.
- Remoundaki, E., Argyraki, A., and Katsiri, A. (2016). Groundwater deterioration: the simultaneous effects of intense agricultural activity and heavy metals in soil. *Procedia Engineering*, 162, 545-552.
- Saadi, R., Saadi, Z., Fazaeli, R., and Fard, N. E. (2015). Monolayer and multilayer adsorption isotherm models for sorption from aqueous media. *Korean Journal of Chemical Engineering*, 32, 787-799.
- Sadasivuni, K. K., Panchal, H., Awasthi, A., Israr, M., Essa, F. A., Shanmugan, S., Suresh, M., Priya, V., and Khechekhouche, A. (2022). Ground water treatment using solar radiation-vaporization and condensation-techniques by solar desalination system. *International Journal of Ambient Energy*, 43(1), 2868-2874.
- Theydan, S. K. A., Bensalah, N., and Khazaei, H. (2012). Adsorption of methylene blue onto biomass-based activated carbon by FeCl₃ activation: Equilibrium, kinetics, and thermodynamic studies. *Journal of Analytical and Applied Pyrolysis*, 97, 116-122.
- Toor, M., Jin, B., Dai, S., Vimonses, V., and Yu, Q. (2012). Adsorption characteristics, isotherm, kinetics, and diffusion of modified natural bentonite for removing diazo dye. *Chemical Engineering Journal*, 187, 79-88.
- Wakeel, A., Siddiqi, E. H., and Tischner, R. (2011). Potassium substitution by sodium in plants. *Critical Reviews in Plant Sciences*, 30(4), 401-413.
- Zamanzadeh-Nasrabadi, S. M., Mohammadiapanah, F., Hosseini-Mazinani, M., and Sarikhan, S. (2023). Salinity stress endurance of the plants with the aid of bacterial genes. *Frontiers in Genetics*, 14, 1049608.